Optical Materials 77 (2018) 211–220

Contents lists available at ScienceDirect

Optical Materials

journal homepage: www.elsevier.com/locate/optmat

Photophysical and electrochemical properties of organic molecules: Solvatochromic effect and DFT studies

Makesh Mohan [a, *], Srikala Pangannaya [b], M.N. Satyanarayan [a], Darshak R. Trivedi [b]

[a] Optoelectronics Laboratory, Department of Physics, National Institute of Technology Karnataka (NITK), Surathkal, Mangalore, 575025, India
[b] Supramolecular Chemistry Laboratory, Department of Chemistry, National Institute of Technology Karnataka (NITK), Surathkal, Mangalore, 575025, India

ARTICLE INFO

Article history:
Received 1 September 2017
Received in revised form
4 January 2018
Accepted 22 January 2018

Keywords:
Schiff base
Photoluminescence
Lifetime
Solvatochromism
DFT

ABSTRACT

A series of five Schiff base molecules **M1**, **M2**, **M3**, **M4** and **M5** have been designed and synthesized by aldol condensation reaction. Synthesized molecules have been characterized by standard spectroscopic techniques in order to confirm their structural traits. The solvatochromic behavior of molecules **M1** to **M5** in solvents of varying polarity were investigated by UV–Vis, fluorescence spectroscopy and supported by TD-DFT calculations. DFT studies performed in the gas phase confirmed the energy stabilized structure of the molecules **M1** to **M5.** Structural characteristics of molecule **M2** favored higher fluorescence emission with a quantum yield of 0.35 and a solid-state emission of 512 nm. Fluorescence lifetime measurement of the molecules **M1** to **M5** exhibited a lifetime of order 2–5 ns. Overall, molecule **M2** can find its application in organic light emitting diodes as a non-dopant emitter material.

1. Introduction

The design and synthesis of organic luminescent materials have attracted considerable attention in academic and industrial circles ever since the pioneering work of Tang et al. in 1987 [1]. Extensive research by the scientific community have unveiled the wide range of applications of organic luminescent materials such as organic light-emitting diodes (OLEDs) [2–5], light-emitting electrochemical cells (LECs) [6,7], triplet–triplet annihilation based upconversion [8–10], fluorescence probes [11–19], therapy [20,21], and bio-imaging [22–25]. OLEDs have thrived in the field of organic electronics leading to practical applications such as flat-panel displays and solid-state lighting resources, due to their low cost [26–28]. Most widely used organic luminescent material is composed of a polycyclic aromatic molecule with one plane of π-conjugated system, which would be favorable to the larger wavelength of absorption (λ_{abs}) and emission (λ_{em}) bands with the stronger absorption intensity and higher luminescence quantum yield (Φ). Nevertheless, luminescence is often weakened or quenched at high concentration or in solid state induced by the phenomenon of aggregation-caused quenching (ACQ) effect [27] that is usually arisen from the intermolecular π–π stacking interactions of π-conjugated plane molecules. ACQ effect is more severe and challenging for OLED applications owing to the presence of luminophores in solid state. More recently, Tang et al. have discovered a phenomenon opposed to ACQ effect known as phenomenon of aggregation-induced emission (AIE) [28]. AIE active materials have seen progressive path in the field of organic electronics and has attracted great research interest [29–32].

Organic functional materials, by virtue of their ease of processing and tunability of properties through a simple chemical modification, lead to myriads of applications in comparison with inorganic materials. The incorporation of functional groups in organic materials have enriched the molecular materials with unique and interesting optoelectronic properties [33–35]. Gondek and co-workers have investigated the effect of nitrogen and methyl substituent on the photophysical properties of organic molecules [36]. Kouari and coworkers have studied the effect of hydroxyl and methoxyl substituents on anthocyanidin and their effect on UV–Vis absorption spectra, with decreasing bandgap and increasing the ground state dipole moment enhancing NLO coefficient in the system [37]. Small organic molecules possessing electron donor and electron acceptor species have proven to exhibit interesting optical and spectral properties aided by intramolecular charge transfer (ICT). The charge transfer transitions have brought in wide infra of applications in photoelectronic and nonlinear optical

* Corresponding author.
E-mail address: ph14f06.makesh@nitk.edu.in (M. Mohan).

https://doi.org/10.1016/j.optmat.2018.01.031
0925-3467/

devices [38,39], chemical sensing [40] and revealing the photochemical and photobiological processes [41]. Moreover, an azobenzene based iminopyridine ligand has been synthesized by condensation reaction between N,Ndimethyl-4,4′-azodianiline and 2-formylpyridine to study its practical application in the field of non-linear optics [42]. Researchers have investigated structure-property relationship on tetrathiafulvalene–quinones and their effect on third-order optical nonlinearity properties [43]. The unique properties of small organic molecules such as strong solvent polarity dependent changes in their photophysical characteristics have made them quite interesting owing to their resultant large red shifts in their emission spectra, stokes shifts between absorption and fluorescence spectra, significant reduction in the fluorescence quantum yield and lifetime on increasing the solvent polarity [44–46].

Salicylaldehyde derivatives have received considerable attention for their facile preparation, good stabilities, biological activities, and rich photophysical properties. Five derivatives of salicylaldehyde **M1, M2, M3, M4** and **M5** have been designed and synthesized. **M1** possesses salicylaldheyde covalently attached through an imine linkage to benzohyrazide moiety without any ancillary substituent in its structure. **M2** and **M3** possess an additional −OH functionality and an additional benzene ring on benzohydrazide group respectively covalently attached through an imine linkage to salicylaldehyde moiety whereas **M4** comprises of an −OH functionality on the naphthoic hydrazide unit. **M5** comprises of nitro (NO_2) functionality on the benzohydrazide unit at position *para* to the imine linked salicylaldehyde. The aim of the present work is focused towards detailed investigation on the spectral behavior and photophysical properties of Schiff base salicylaldehyde derivatives in solvents of varying polarity. The effect of solvation on the photophysical properties of molecules **M1** to **M5** have been investigated to understand the excited state properties in solvents of varying polarity. It was observed under present study that the presence of ancillary substituent, like −OH, naphthyl and NO_2 had profound influence on the physicochemical properties. UV–Vis absorption studies, photoluminescence studies and cyclic voltammetric studies performed on the molecules reveal the utility in OLED applications. The study of energy band gap of the derivatives through density functional studies (DFT) in support of the experimental techniques has been the main theme of the present work.

2. Experimental

2.1. Materials and methods

All the chemicals used in the present study were procured from Sigma-Aldrich and Alfa Aesar and were used as received without further purification. All the solvents were purchased from SD Fine, India, were of HPLC grade and used without further distillation. Melting point was measured on Stuart SMP3 melting-point apparatus in open capillaries. Infrared spectrum was recorded on Bruker Apex FTIR spectrometer. UV–Vis spectroscopy was performed with analytik jena Specord S600 spectrometer in standard 3.0 mL quartz cell with 1 cm path length. The ^{1}H NMR spectra were recorded on Bruker Ascend (400 MHz) instrument using TMS as internal reference and DMSOd_6 as solvent. Resonance multiplicities are described as s (singlet), d (doublet), t (triplet) and m (multiplet). Cyclic voltammogram was recorded on IVIUM electrochemical workstation (Vertex) at a scan rate of 20 mV/s with the potential range −2.5 V to 2.5 V. DSC was performed using Shimadzu DSC-60. Differential scanning calorimetry calibrated using tin standard material. For the analysis, samples were kept on the aluminum pan and covered with a crimped lid and scanned from 30 °C to 300 °C at a scanning rate of 10 °C/minute under a continuously purged dry nitrogen atmosphere.

2.2. Synthesis

The molecules **M1, M2, M3, M4** and **M5** were synthesized by simple condensation reaction between salicylaldehyde and different substituted hydrazides. Ethanolic solution of salicylaldehyde was slowly added to an ethanolic solution of different substituted hydrazides. The desired products were obtained in a one-step reaction by refluxing in ethanol using acetic acid as catalyst at 78 °C for 4 h. The formation of the product was confirmed through Thin Layer Chromatography (TLC) by the generation of single spot indicative of the disappearance of starting materials. After cooling to room temperature, the reaction mixture was filtered through filter paper, washed with ethanol to obtain pure product. The compounds have been characterized by various spectral techniques such as DSC, FT-IR and ^{1}H NMR analysis. The structures of the molecules **M1** to **M5** are shown in Scheme 1.

M1: (E)-N'-(2-hydroxybenzylidene)benzohydrazide White solid (75%). M.p. 173.06 °C. FT-IR (ATR, cm^{-1}) ν: 3587(OH), 3264 (NH), 1669 (-CH=N-). ^{1}HNMR (400 MHz, DMSOd_6, δ ppm):12.10 (s, NH), 11.31 (s, OH), 8.66 (s, -CH=N), 7.96 (d, 2Ar-H), 7.60 (dt, 4Ar-H), 6.95 (t, Ar-CH), 7.32 (t, 2Ar-H).

M2: (E)-N'-(2-hydroxybenzylidene)-2-hydroxybenzohydrazide Pale yellow solid (82%). M.p. 293 °C. FT-IR (ATR, cm^{-1}) ν: 3686(OH), 3427 (NH), 1612 (-CH=N-). ^{1}HNMR (400 MHz, DMSOd_6, δ ppm): 12.04 (s, NH), 11.77 (s, OH), 11.18 (s, OH), 8.68 (s, -CH=N-), 7.89 (dd, Ar-H), 7.57 (dd, Ar-H), 7.46 (ddd, Ar-H), 7.32 (td, Ar-H), 6.99 (m, Ar-H), 6.95(m, Ar-H).

M3: (E)-N'-(2-hydroxybenzylidene)-1-naphthohydrazide Pale yellow solid (85%). M.p. 242.54 °C. FT-IR (ATR, cm^{-1}) ν: 3649(OH), 3427 (NH), 3001(CH stretching), 1644 (-CH=N-). ^{1}HNMR (400 MHz, DMSOd_6, δ ppm): 12.25 (s, NH), 11.22 (s, OH), 8.55 (s, -CH=N-), 8.25 (m, Ar-H), 8.09 (m, Ar-H), 7.80 (dd, Ar-H), 7.62 (m, 6Ar-H), 7.32 (m, Ar-H), 6.95 (m, 2Ar-H).

M4: (E)-3-hydroxy-N'-(2-hydroxybenzylidene)-2-naphthohydrazide: White solid (77%). M.p. 299.69 °C. FT-IR (ATR, cm^{-1}) ν: 3251(OH), 3165 (NH), 3051(CH stretching), 1642(-CH=N-). ^{1}HNMR (400 MHz, DMSOd_6, δ ppm): 12.16 (s, NH), 11.26 (s, OH), 11.19 (s, OH), 8.68 (s, -CH=N-), 8.46 (s, Ar-H), 7.85 (dd, 2Ar-CH), 7.55 (m, 1Ar-CH), 7.34 (m, 4Ar-H), 6.95 (m, 2Ar-H).

M5: (E)-N'-(2-hydroxybenzylidene)-4-nitrobenzohydrazide Pale yellow solid (83%). M.p. 299.58 °C. FT-IR (ATR, cm^{-1}) ν: 3215 (OH), 3062 (NH), 3001(CH stretching), 1647 (-CH=N-). ^{1}HNMR (400 MHz, DMSOd_6, δ ppm): 12.36 (s, NH), 11.09 (s, OH), 8.69 (s, -CH=N), 8.39 (d, 2Ar-H), 8.18 (d, 2Ar-H), 7.61 (m, Ar-H), 7.32 (t, Ar-H), 6.94 (m, Ar-H).

3. Results and discussion

3.1. UV–Vis studies and solvent effect

The optical properties of synthesized molecules were studied in order to probe the influence of substituents such as extension of π conjugation or increasing donor character on the photophysical properties of salicylaldehyde derivatives. With a view to evaluate the effect of polarities and hydrogen bond forming abilities of various organic solvents on the fluorescence and absorption spectra of molecules, UV–Vis spectra and fluorescence spectra of **M1** to **M5** have been recorded. 10^{-5} M solution of the molecules were prepared in solvents of varying polarity such as THF, DCM, acetone, EtOH, ACN, DMF and DMSO. Molecules **M2** and **M4** exhibited significant fluorescence in solution phase when illuminated with UV lamp as shown in Fig. 1.

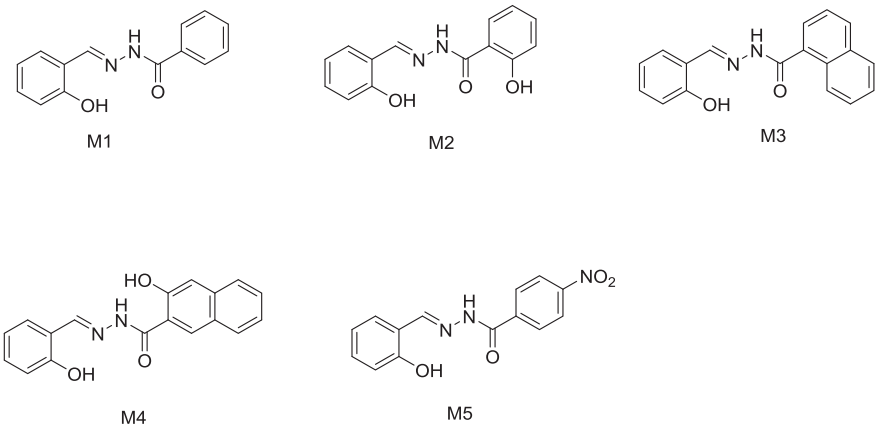

Scheme 1. 1. Structure of molecules **M1, M2, M3, M4** and **M5**.

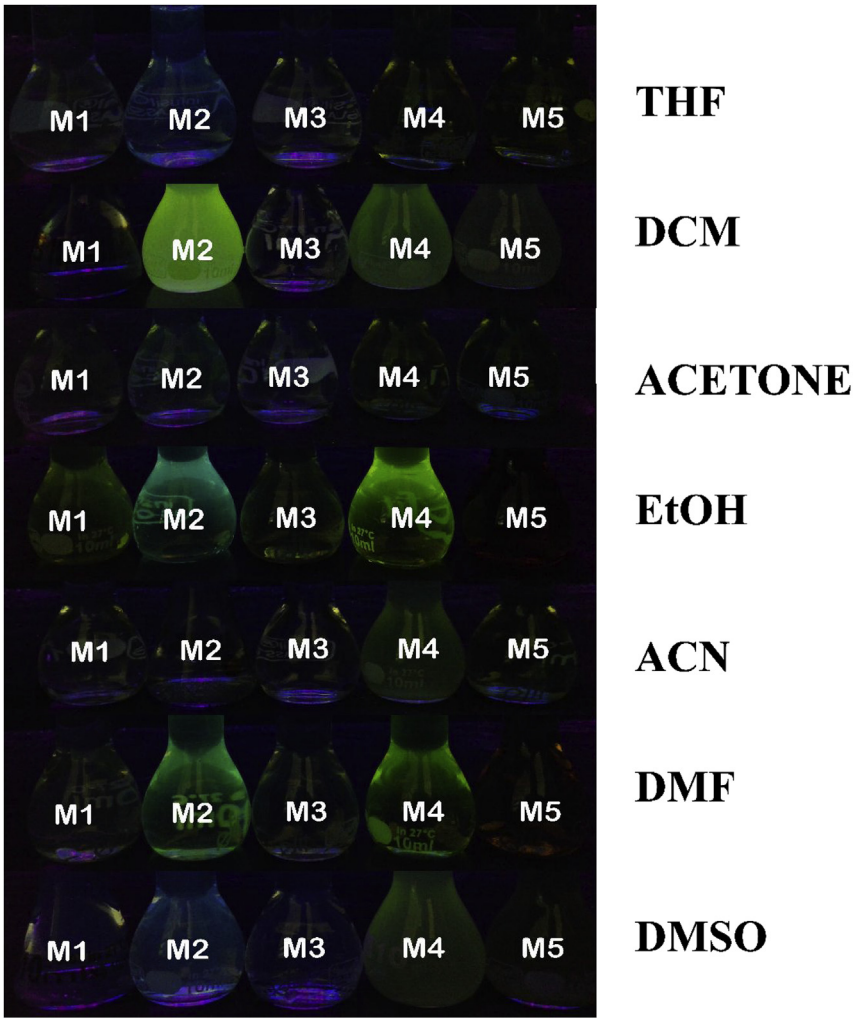

Fig. 1. Fluorescent response of molecules **M1** to **M5** (10^{-5} M) in solvents of varying polarity under UV illumination.

The UV–Vis spectra of these molecules reveal that the absorption band in the region ~300 nm corresponds to the transition between the p-orbital localized on the central bond of azomethine (HC=N-) and the carbonyl (C=O) group. The second band located in the range of ~350–400 nm refers to an intramolecular charge transfer (CT) transition within the molecule [47]. Furthermore, the band at 400 nm is highly significant in salicylaldimine derivatives which indicate the occurrence of strong intramolecular hydrogen bond between the hydroxyl group and the azomethine nitrogen that causes planarity of the molecules. This further facilitates the charge transfer bands which are more sensitive to solvent changes than bands which are resulting from local transition [47]. The results are shown in Table 1.

The role of solvent is significant in spectroscopic analysis as it induces predominant changes in the position, intensity and shape of the absorption and fluorescence bands [48]. The effect of changes in the polarity of the solvents is reflected in changes in the excitation and emission wavelengths on whether S1 or S0 is more stabilized by the solvent [49]. Among all the solvents used in the present study, each molecule showed highest Stokes shift values in a specific solvent. This reveals the influence of solvent polarity in promoting or nullifying the solute-solvent interactions. 10^{-5} M solution of molecule **M1** in DMSO, **M2** in EtOH, **M3** and **M4** in DMF and **M5** in ACN exhibited maximum stokes shift differing by 223, 162, 165, 188 and 111 units respectively. This proved the complex nature of solute solvent interactions dominated by the hydrogen bond accepting nature of the solvents to have a prominent role in inducing red shift. The red shift and the stokes shift observed for the molecules with the increase in solvent polarity reveals that the long wavelength band of the molecule is due to n-π^* transitions existing in the neutral molecules used in the present study.

Table 1
Photophysical aspects of molecules **M1** to **M5** in solvents of varying polarity.

	λ_{abs} (nm)	λ_{ex} (nm)	λ_{ems} (nm)	Stoke Shift	FWHM
Tetrahydrofuran					
M1	334, 295, 250	250	306	56	34
M2	334, 295, 250	334	446	112	75
M3	334, 295, 250	334	436	102	69
M4	335, 305, 295, 250	250	311	61	38
M5	338, 295, 250	250	311	61	39
Dichloromethane					
M1	330, 294, 285	294	392	98	99
M2	335, 293	293	392	99	102
M3	328, 294	294	393	99	103
M4	334, 308	308	394	86	59
M5	340, 292	292	393	101	78
Acetone					
M1	345, 415	345	426	81	79
M2	331	331	484	153	150
M3	343	343	428	85	124
M4	350	350	513	163	86
M5	350	350	427	77	77
Ethanol					
M1	400, 330, 296, 285	330	429	99	68
M2	400, 333, 301	301	463	162	80
M3	400, 329, 297	329	429	100	65
M4	400, 337, 275	400	557	157	125
M5	345	345	430	85	64
Acetonitrile					
M1	3,33,29,52,85,271	271	373	102	105
M2	3,35,291	335	474	139	102
M3	3,32,294	294	376	82	121
M4	33,93,03,290	290	360	70	121
M5	33,92,90,267	267	378	111	96
n,n-dimethylformamide					
M1	397, 329, 298, 286	397	458, 553	61, 156	105
M2	412, 381, 364, 330	330	455	125	82
M3	395, 329, 300	395	560	165	95
M4	340	340	528	188	104
M5	380, 357	380	453	73	73
Dimethylsulfoxide					
M1	329, 299, 288	329	552	223	175
M2	385, 329	385	458	73	78
M3	329, 285	285	336	51	51
M4	400, 333, 276	400	557	157	104
M5	342, 276	276	330	54	55

The UV–Vis spectral studies of the molecules **M1** to **M5** in solvents of varying polarity reveals the following results. The molecules **M1** and **M5** exhibited linear correlation between the solvent polarity and red shift in the absorption bands in solvents such as THF, DCM and acetone. The absorption band for **M1** and **M5** exhibited a red shift in solvents of increasing polarity following an order THF < DCM < acetone differing by 50 units respectively. THF and acetone being polar aprotic solvents, DCM being a non-polar solvent exhibited less prevalent solute-solvent interactions on the molecules. Molecules **M1** and **M5** did not exhibit any linear correlation between solvent polarity and red shift in absorption band in solvents of higher dielectric constants such as EtOH, DMF, ACN, and DMSO. The UV–Vis spectra of molecules **M1** and **M5** are represented in Figs. S12 and S15 (Supplementary data). Ethanol being a polar protic solvent, DMF, ACN and DMSO being polar aprotic solvent introduced complex nature of solute solvent interactions dominated by the hydrogen bond accepting nature of the solvents. The hydrogen bonding capacity of the solvents is necessary to be considered from a view point of its importance over polarity. This is justified with the anomalous behavior observed in the case of ACN which is more polar than DMF, yet exclusively a hydrogen-bond acceptor. Molecules **M2**, **M3** and **M4** by virtue of the presence of an additional –OH functionality did not show any linear dependence on the solvent polarity and the red shift, yet indicating complex nature of solute solvent interactions. This justifies the role of –OH functionality as a hydrogen bond donor site aiding the solute-solvent interactions with hydrogen bond acceptor solvents such as DMSO, ACN and EtOH. The UV–Vis spectra of molecules **M2**, **M3** and **M4** are represented in Fig. 2, Fig. S13 (Supplementary data) and Fig. S14 (Supplementary data) respectively. Molecules **M2** and **M4**, possessing two –OH functionalities, exhibited a significant red shift at 385 nm and 400 nm respectively in DMSO which is attributed to the hydrogen bond interactions dominating over the solute-solvent interactions.

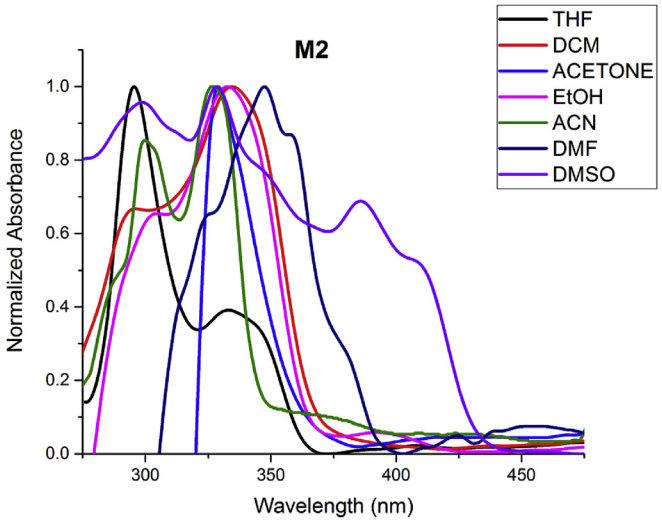

Fig. 2. UV–Vis spectra of molecule **M2** in solvents of varying polarity.

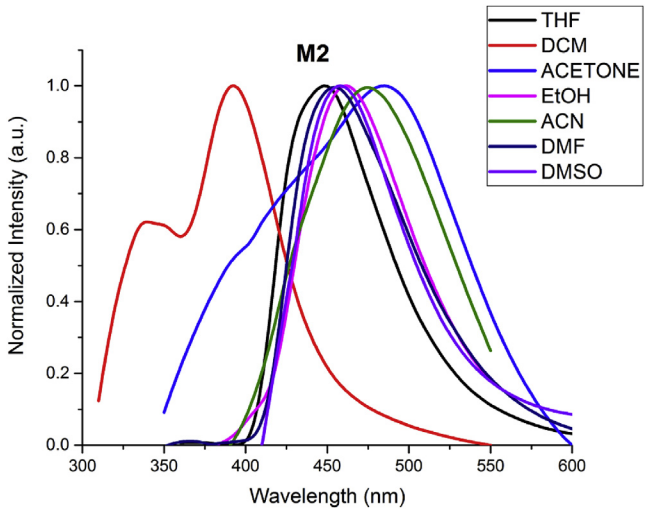

Fig. 3. Photoluminescence spectra of molecule **M2** in solvents of varying polarity.

3.2. Photoluminescence studies

Photoluminescence studies were performed for the molecules **M1** to **M5** in solvents of varying polarity. Furthermore, all the materials show good solvatochromic effect in wide range of solvent polarities. The probability of absorption is greater in polar solvents in contrast with the fluorescence intensity which is affected by other processes such as internal conversion and intersystem crossing. These processes are favored by greater hydrogen bond accepting character of ACN relative to other polar and hydrogen-bond donor solvents such as methanol which inhibit these non-radiative processes. Fluorescence emission is favored in solvents of higher dielectric constants such EtOH and DMF. **M2**, by virtue of the presence of two OH functionalities which is in direct conjugation with the imine linkage, further favors delocalization of electrons. This in turn influences the electronic transition in the molecule leading to emission intensity greater in comparison with the other molecules of the series. The fluorescence emission spectrum of **M2** in various solvents is represented in Fig. 3. Variation of emission wavelengths of the molecules **M1** to **M5** in solvents of varying polarity is shown in Fig. 4. Further, emission spectra of molecules **M1**, **M3**, **M4** and **M5** is given in Fig. S21-S24 (Supplementary data).

3.3. Fluorescence lifetime studies

Measurement of the fluorescence lifetime have been performed with standard time-correlated single-photon counting method (TCSPC). An LED with an excitation wavelength of 346 nm and a spectral width of 1.2 nm has been used to excite the molecules. The lifetime curves for **M1** to **M5** are represented in Fig. 5. The decay curves obtained are then fitted with a DAS6 software to obtain the fluorescence lifetime of the molecules (τ_s) and the results are tabulated in Table 2. In general, certain materials exhibit only first order progression decay having a single lifetime component, and other materials can exhibit second or third order progression decay, resulting in two or three component lifetimes [50]. Decay curve with a good fit resulted in a XSQR value of lesser than 1.2 for the molecules **M1**, **M2** and **M3** with a three-component lifetime and a two-component lifetime for molecules **M4** and **M5**.

3.4. Fluorescence quantum yield determination

The fluorescence quantum yield (ϕ_f) were evaluated according to the following equation, where Coumarin 153 in cyclohexane was

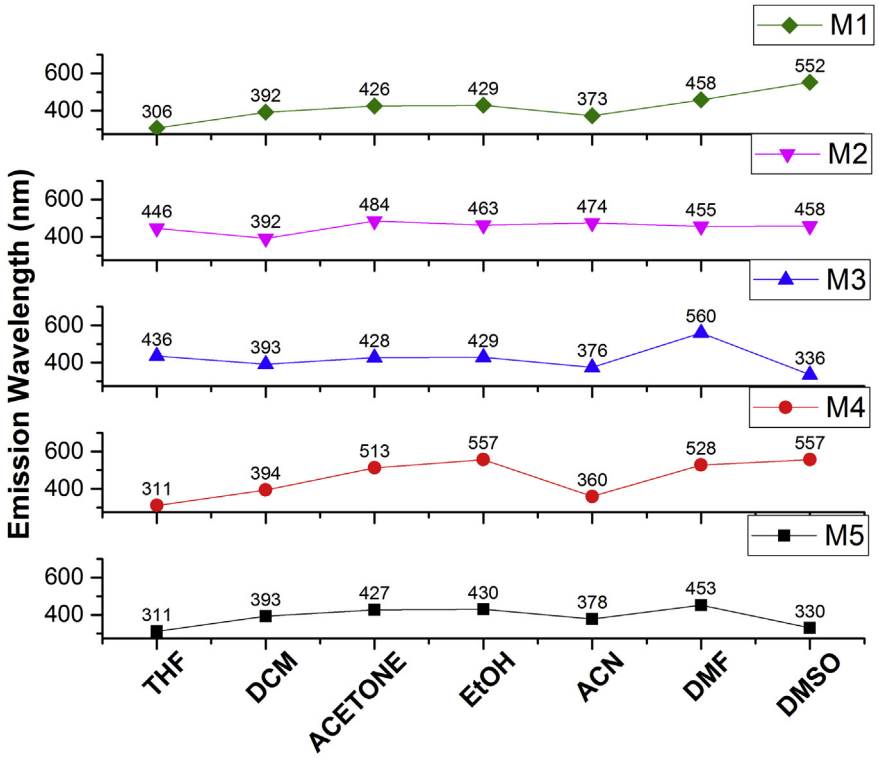

Fig. 4. Variation in the emission wavelength of molecules **M1** to **M5** in solvents of varying polarity.

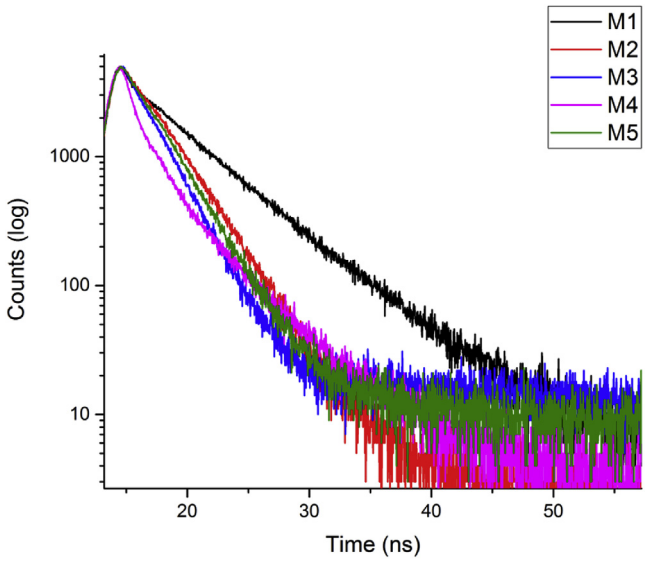

Fig. 5. Fluorescence decay curve of molecules **M1** to **M5** excited with a source of 346 nm.

Table 2
The lifetime of molecules **M1** to **M5** and its XSQR value.

Molecule	XSQR	Lifetime (ns)		
		T1	T2	T3
M1	1.095	1.3	5.59	0.079
M2	1.184	1.63	2.91	0.0763
M3	1.069	0.163	1.65	2.69
M4	1.063	0.78	4.39	–
M5	1.053	0.982	2.59	–

used as a reference (R) for molecule **M2** and quinine sulphate in 0.5 M H_2SO_4 chosen as the reference (R) for other molecules in the series. Molecules **M1** to **M5** whose quantum yield to be determined is denoted as S. Grad corresponds to the gradient from the plot of integrated fluorescence intensity vs absorbance at the excitation wavelength, and η the refractive index of the solvent for standard and reference [51,52]. Molecule **M2** exhibited a highest quantum yield value of 0.35 in DMSO, whereas molecules **M1** and **M4** showed a quantum yield value of 0.005 and 0.06. The estimated quantum yield of the molecules is presented in Table 3. Further there were no significant emissions from **M3** and **M5** with reference to the standard.

$$\varphi_S = \varphi_R \left[\frac{Grad_S}{Grad_R}\right] \frac{\eta_S^2}{\eta_R^2} \quad (1)$$

3.5. Solid state photoluminescence studies

Molecules **M1** to **M5** were deposited onto chemically cleaned glass substrates with the help of thermal vacuum deposition to study its solid-state emission properties. Molecule **M2** exhibited higher emission intensity in solid state in comparison with the solution state exhibiting aggregation induced emission. **M4** exhibited a mild emission as compared to **M2** as shown in Fig. 6. The -OH functionality in **M2** and **M4** are known to have prominent role in exhibiting solid state luminescent property. **M1** and **M3** devoid of -OH substitution on one of the aromatic counterpart did not exhibit solid state emission. Further, molecule **M5**, due to the presence of -NO_2 group quenched the emission intensity and hence no significant solid-state emission was observed. Photoluminescence spectra of the molecules **M2** and **M4** are as given in Fig. 7 with the photophysical parameters tabulated in Table 4.

Molecule **M2** exhibited a solid-state emission at 512 nm red shifted in comparison with the solution state whereas **M4** exhibited an emission at 520 nm with a FWHM of 88. A good color purity would imply in achieving a value of FWHM lesser than 60 and molecule **M2** exhibited a value of 70. Overall, molecule **M2** exhibited a good solid-state emission property finding its utility as emitter material in OLEDs.

3.6. Cyclic voltammetric studies

Cyclic voltammetric studies of molecules have been performed with three electrode cell in ACN medium and tetrabutylammonium perchlorate as supporting electrolyte. The anodic peak corresponds to the oxidation of –NH functionality and the cathodic peak corresponds to the reduction of keto (C=O) functionality. Molecule **M5** has a NO_2 and a keto functionality which can undergo reduction. The cyclic voltammogram is represented in Fig. 8. Further, the onset potentials of oxidation and reduction of a material can be correlated to the ionization potential (I_p) and electron affinity (E_a) according to

Table 3
Measured quantum yield for molecules **M1, M2** and **M4**.

Molecule	**M1**	**M2**	**M3**	**M4**	**M5**
ϕ_f	0.005	0.35	ND[a]	0.06	ND[a]

[a] ND – not determined (emission intensity is very low in comparison with standard).

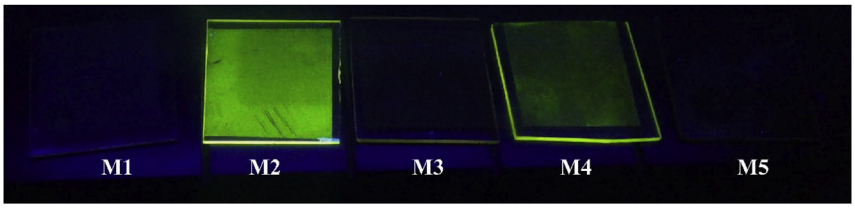

Fig. 6. Solid-state emission of molecules **M1** to **M5** observed under UV lamp.

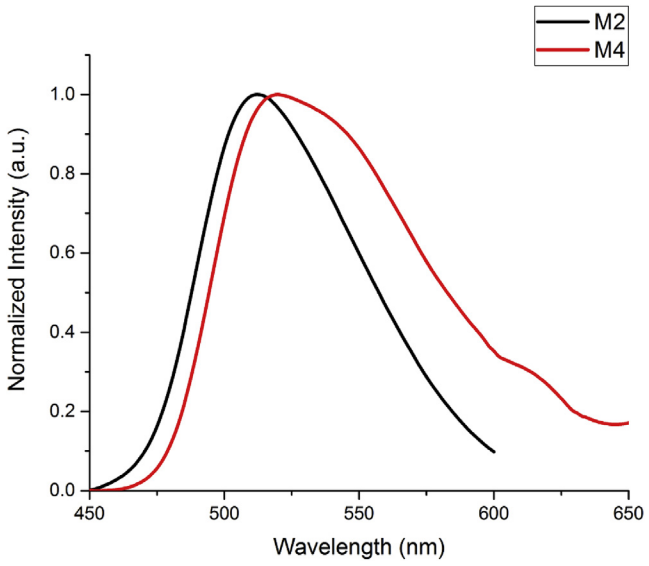

Fig. 7. Solid-state photoluminescence spectra of molecule **M2** and **M4**.

Table 4
Photoluminescence parameters of molecules **M2** and **M4** in solid state.

Molecule	λ_{ex} (nm)	λ_{ems} (nm)	Stokes Shift	FWHM
M2	360	512	152	70
M4	350	520	170	88

the empirical relationship proposed by Bredas and co-workers on the basis of a detailed comparison between valence effective Hamiltonian calculations and experimental electrochemical measurements [53]. The highest occupied molecular orbital (HOMO) and the lowest unoccupied molecular orbital (LUMO) have been calculated [54] by using Eqs. (2) and (3) and the energy band gap E_g deduced from Eq. (4) for the molecules are represented in Fig. 9. The estimated value of HOMO and LUMO for molecules **M1** to **M5** is tabulated in Table 5.

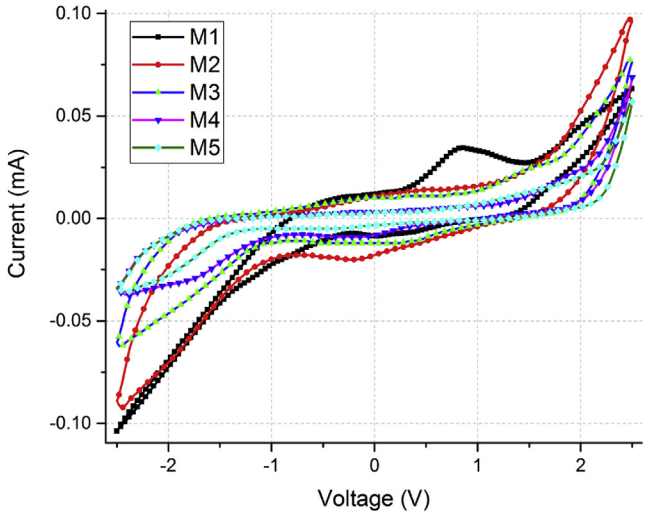

Fig. 8. Cyclic voltammogram of molecules **M1** to **M5**.

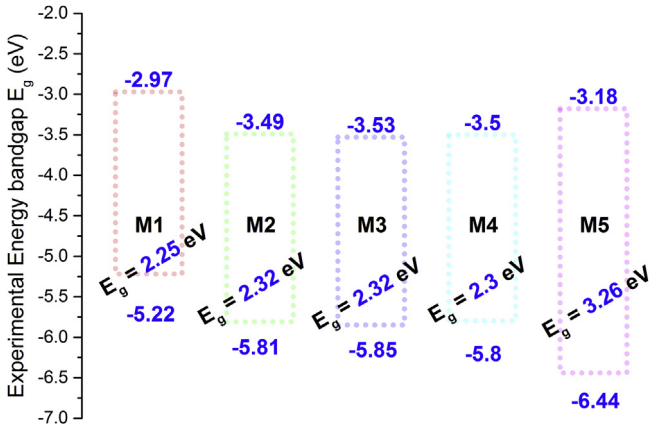

Fig. 9. HOMO, LUMO and band gap of molecule **M1** to **M5** derived from cyclic voltammetry.

$$I_p = -(E_{ox} + 4.4)eV \quad (2)$$

$$E_a = -(E_{red} + 4.4)eV \quad (3)$$

$$E_g = E_a - I_p \quad (4)$$

3.7. DFT studies

The geometrical and electronic properties of molecules **M1** to **M5** were performed using Gaussian 09 package [55]. The geometry optimization was achieved by means of B3LYP (Becke three parameters hybrid functional with Lee-Yang-Perdew correlation functionals) [56,57] with the 6-311++G (d, p) basis set [58,59]. The molecules **M1** to **M5** with their optimized geometry and their dihedral angle is shown in Fig. 10. Highest occupied molecular orbitals and lowest unoccupied molecular orbitals were visualized using Avogadro software [60,61]. Vertical transition energies of singlet excited states in gas phase was estimated. Oscillator strength for all the structures were estimated using time-dependent DFT method (TD-DFT) at the same level of calculation with the same basis set that was used for ground state optimization.

3.7.1. Time dependent density functional theory (TD-DFT)

TD-DFT calculation under the same basis set with vertical transition energies up to first 20 singlet excited states for all the molecules under various solvents have been estimated. The effect of solvent on the energy parameters has been incorporated by self-

Table 5
Estimation of HOMO, LUMO and bandgap of molecules **M1** to **M5** from electrochemical studies.

Molecule	I_{ox} (V)[a]	E_{red} (V)[b]	E_{HOMO} (eV)	E_{LUMO} (eV)	E_g (eV)
M1	0.82	−1.43	−5.22	−2.97	2.25
M2	1.41	−0.91	−5.81	−3.49	2.32
M3	1.45	−0.87	−5.85	−3.53	2.32
M4	1.4	−0.9	−5.8	−3.5	2.3
M5	2.04	−1.22	−6.44	−3.18	3.26

[a] Oxidation onset measured from cyclic voltammogram.
[b] Reduction onset measured from cyclic voltammogram.

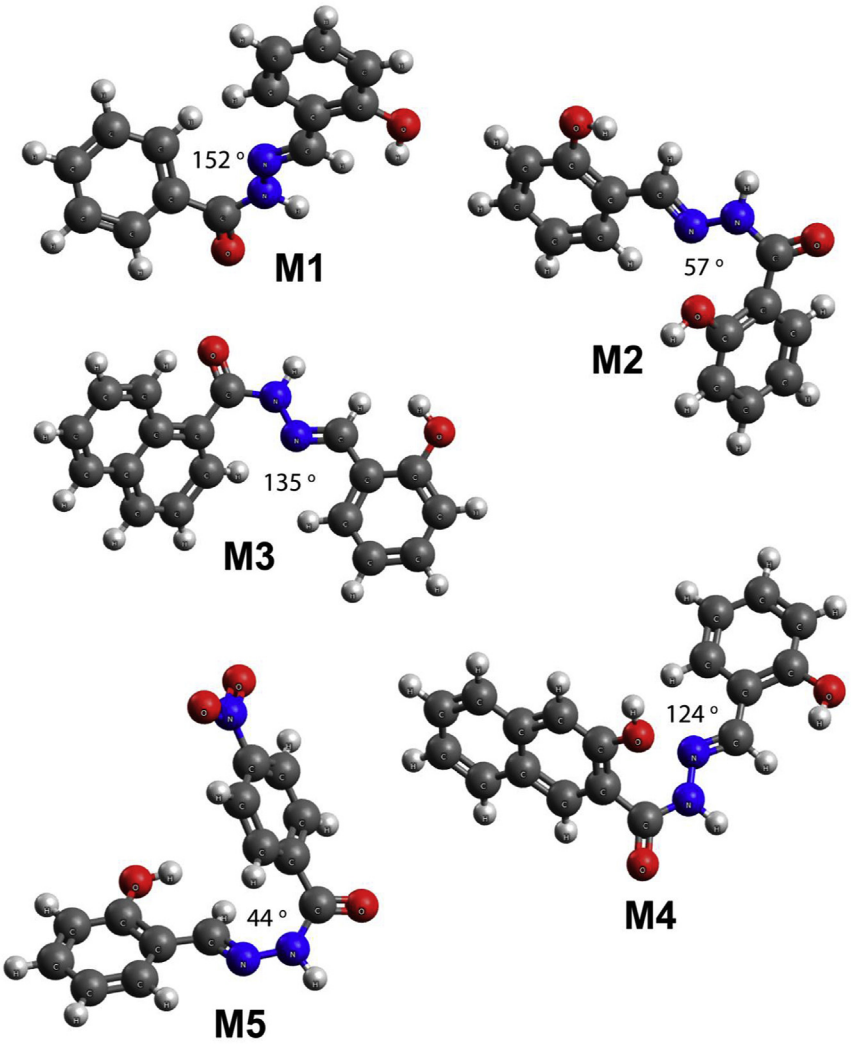

Fig. 10. DFT optimized structures of the molecules **M1** to **M5**.

consistent reaction field using inbuilt conductor polarizable continuum model (SCRF-CPCM) [62] as implemented in Gaussian09 software. The energy distribution diagram in gas phase representing HOMO and LUMO is shown in Fig. 11. Molecules **M1** to **M4** have their LUMO energy distributed on the entire molecule except for **M5** where it is localized on nitro benzohydrazide moiety. HOMO is localized on salicylaldehyde and the imine group for molecules **M1**, **M2** and **M5**, whereas it is delocalized on the entire molecule for **M3** and localized on naphthohydrazide for **M4**. Charge transfer transition is occurring between the salicylaldehyde and the entire molecular network as seen in the spatial distribution. The corresponding UV–Vis spectra are represented in Fig. S16-S20 (Supplementary data). Computed electronic transitions obtained for the molecules **M1** to **M5** were in good agreement with the experimentally obtained absorbance. The overall trend of the spectrum remained the same in comparison with the experimental results where the discrepancies seen in the energy transition may be attributed to the theoretical overestimation.

4. Conclusions

Molecules **M1** to **M5** have been synthesized in good yield and characterized by standard spectroscopic techniques like FT-IR, ^{1}H-NMR and DSC. Solvent dependent studies of molecules **M1** to **M5** exhibited meager linear correlation between the solvent polarity and the observed red shift value. This confirmed the solute-solvent interaction dominating over the hydrogen bond accepting nature of the solvents. Bandgap determination of the molecules **M1** to **M5** was measured experimentally from the cyclic voltammetric studies. Energetically optimized ground state and the excited state structure obtained from DFT and TD-DFT correlates with the experimental results. The photophysical properties evaluated by UV–Vis, photoluminescence, lifetime and quantum yield studies have paved a way to look into the device applications in the field of OLED. Overall, spectroscopic studies reveal molecule **M2** as a promising candidate for green OLED device applications. Further OLED device application of these molecules will be studied and presented in the future work.

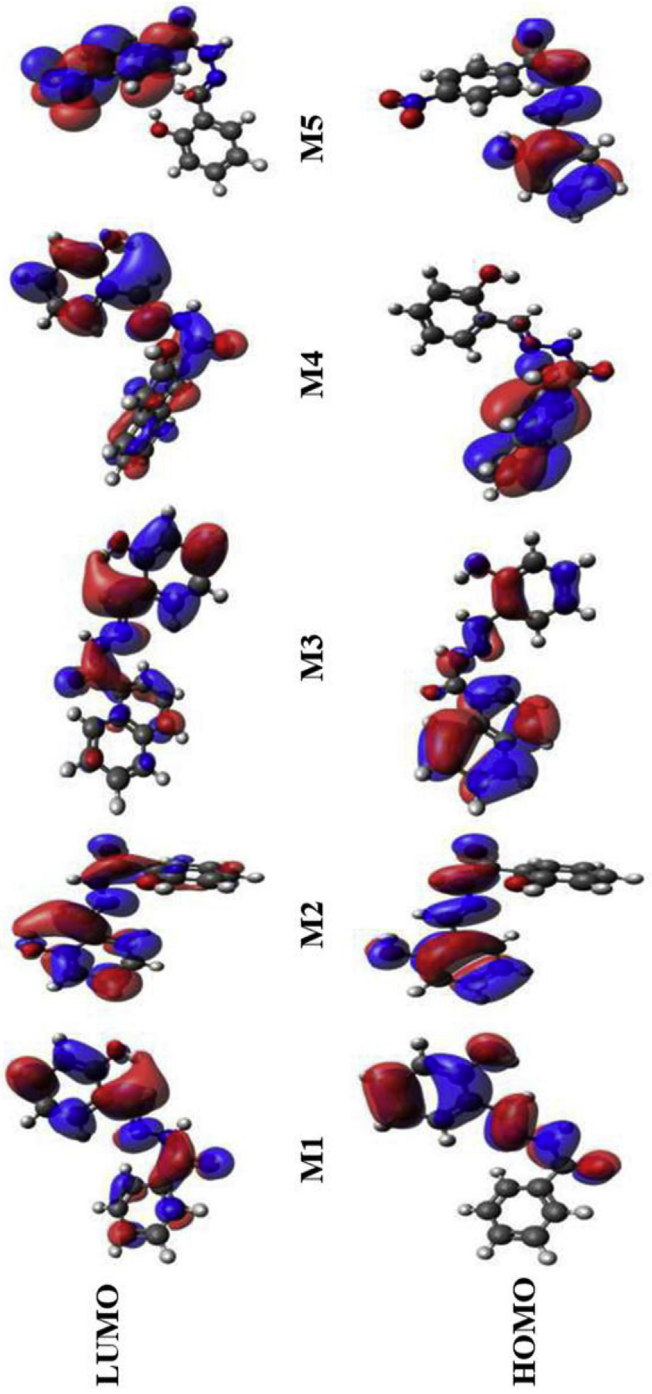

Fig. 11. Representation of energy distribution in molecules **M1** to **M5** in gas phase.

Acknowledgement

MM and SP are thankful to NITK, Surathkal for the research fellowship and providing the research infrastructure. MM is thankful to TEQIP II for providing the photoluminescence characterization facility. We are thankful to IISc Bangalore for NMR analysis. MM is thankful to Dr. Ajith K M, Assistant professor, Department of Physics, NITK, Surathkal for his support in providing access to Gaussian 09 package.

Appendix A. Supplementary data

Supplementary data related to this article can be found at https://doi.org/10.1016/j.optmat.2018.01.031.

References

[1] C.W. Tang, S.A. VanSlyke, Organic electroluminescent diodes, Appl. Phys. Lett. 51 (1987) 913–915, https://doi.org/10.1063/1.98799.
[2] U. Mitschke, P. Bäuerle, The electroluminescence of organic materials, J. Mater. Chem. 10 (2000) 1471–1507, https://doi.org/10.1039/A908713C.
[3] L.S. Hung, C.H. Chen, Recent progress of molecular organic electroluminescent materials and devices, Mater. Sci. Eng. R Rep. 39 (2002) 143–222, https://doi.org/10.1016/S0927-796X(02)00093-1.
[4] H. Yersin, Highly Efficient OLEDs with Phosphorescent Materials, John Wiley & Sons, 2008.
[5] H. Xiang, J. Cheng, X. Ma, X. Zhou, J.J. Chruma, Near-infrared phosphorescence: materials and applications, Chem. Soc. Rev. 42 (2013) 6128–6185, https://doi.org/10.1039/C3CS60029G.
[6] J.D. Slinker, J. Rivnay, J.S. Moskowitz, J.B. Parker, S. Bernhard, H.D. Abruña, G.G. Malliaras, Electroluminescent devices from ionic transition metal complexes, J. Mater. Chem. 17 (2007) 2976–2988, https://doi.org/10.1039/B704017B.
[7] R.D. Costa, E. Ortí, H.J. Bolink, Recent advances in light-emitting electrochemical cells, Pure Appl. Chem. 83 (2011) 2115–2128, https://doi.org/10.1351/PAC-CON-11-07-20.
[8] T.N. Singh-Rachford, F.N. Castellano, Photon upconversion based on sensitized triplet–triplet annihilation, Coord. Chem. Rev. 254 (2010) 2560–2573, https://doi.org/10.1016/j.ccr.2010.01.003.
[9] J. Zhao, S. Ji, H. Guo, Triplet–triplet annihilation based upconversion: from triplet sensitizers and triplet acceptors to upconversion quantum yields, RSC Adv. 1 (2011) 937–950, https://doi.org/10.1039/C1RA00469G.
[10] J. Zhao, W. Wu, J. Sun, S. Guo, Triplet photosensitizers: from molecular design to applications, Chem. Soc. Rev. 42 (2013) 5323–5351, https://doi.org/10.1039/C3CS35531D.
[11] R. Martínez-Máñez, F. Sancenón, Fluorogenic and chromogenic chemosensors and reagents for anions, Chem. Rev. 103 (2003) 4419–4476, https://doi.org/10.1021/cr010421e.
[12] E.M. Nolan, S.J. Lippard, Tools and tactics for the optical detection of mercuric ion, Chem. Rev. 108 (2008) 3443–3480, https://doi.org/10.1021/cr068000q.
[13] H.N. Kim, M.H. Lee, H.J. Kim, J.S. Kim, J. Yoon, A new trend in rhodamine-based chemosensors: application of spirolactam ring-opening to sensing ions, Chem. Soc. Rev. 37 (2008) 1465–1472, https://doi.org/10.1039/B802497A.
[14] Q. Zhao, F. Li, C. Huang, Phosphorescent chemosensors based on heavy-metal complexes, Chem. Soc. Rev. 39 (2010) 3007–3030, https://doi.org/10.1039/B915340C.
[15] J.F. Zhang, Y. Zhou, J. Yoon, J.S. Kim, Recent progress in fluorescent and colorimetric chemosensors for detection of precious metal ions (silver, gold and platinum ions), Chem. Soc. Rev. 40 (2011) 3416–3429, https://doi.org/10.1039/C1CS15028F.
[16] K. Kaur, R. Saini, A. Kumar, V. Luxami, N. Kaur, P. Singh, S. Kumar, Chemodosimeters: an approach for detection and estimation of biologically and medically relevant metal ions, anions and thiols, Coord. Chem. Rev. 256 (2012) 1992–2028, https://doi.org/10.1016/j.ccr.2012.04.013.
[17] Y. Feng, J. Cheng, L. Zhou, X. Zhou, H. Xiang, Ratiometric optical oxygen sensing: a review in respect of material design, Analyst 137 (2012) 4885–4901, https://doi.org/10.1039/C2AN35907C.
[18] Y. Yang, Q. Zhao, W. Feng, F. Li, Luminescent chemodosimeters for bioimaging, Chem. Rev. 113 (2013) 192–270.
[19] J. Cheng, X. Zhou, H. Xiang, Fluorescent metal ion chemosensors via cation exchange reactions of complexes, quantum dots, and metal–organic frameworks, The Analyst 140 (2015) 7082–7115, https://doi.org/10.1039/C5AN01398D.
[20] R.W.-Y. Sun, C.-M. Che, The anti-cancer properties of gold(III) compounds with dianionic porphyrin and tetradentate ligands, Coord. Chem. Rev. 253 (2009) 1682–1691, https://doi.org/10.1016/j.ccr.2009.02.017.
[21] L. Feng, C. Zhu, H. Yuan, L. Liu, F. Lv, S. Wang, Conjugated polymer nanoparticles: preparation, properties, functionalization and biological applications, Chem. Soc. Rev. 42 (2013) 6620–6633, https://doi.org/10.1039/C3CS60036J.
[22] V. Fernández-Moreira, F.L. Thorp-Greenwood, M.P. Coogan, Application of d6 transition metal complexes in fluorescence cell imaging, Chem. Commun. 46 (2009) 186–202, https://doi.org/10.1039/B917757D.
[23] Q. Zhao, C. Huang, F. Li, Phosphorescent heavy-metal complexes for bioimaging, Chem. Soc. Rev. 40 (2011) 2508–2524, https://doi.org/10.1039/C0CS00114G.
[24] G. Mallesham, S. Balaiah, M.A. Reddy, B. Sridhar, P. Singh, R. Srivastava, K. Bhanuprakash, V.J. Rao, Design and synthesis of novel anthracene derivatives as n-type emitters for electroluminescent devices: a combined experimental and DFT study, Photochem. Photobiol. Sci. 13 (2014) 342–357, https://doi.org/10.1039/C3PP50284H.

[25] M. Zhu, C. Yang, Blue fluorescent emitters: design tactics and applications in organic light-emitting diodes, Chem. Soc. Rev. 42 (2013) 4963–4976, https://doi.org/10.1039/C3CS35440G.
[26] S.-J. Yoo, H.-J. Yun, I. Kang, K. Thangaraju, S.-K. Kwon, Y.-H. Kim, A new electron transporting material for effective hole-blocking and improved charge balance in highly efficient phosphorescent organic light emitting diodes, J. Mater. Chem. C 1 (2013) 2217–2223, https://doi.org/10.1039/C3TC00801K.
[27] G. v. Bünau, J.B. Birks, Photophysics of aromatic molecules, Wiley-Interscience, London 1970. 704 Seiten. Preis: 210s, Berichte Bunsenges, Für Phys. Chem. 74 (1970) 1294–1295, https://doi.org/10.1002/bbpc.19700741223.
[28] J. Luo, Z. Xie, J.W.Y. Lam, L. Cheng, H. Chen, C. Qiu, H.S. Kwok, X. Zhan, Y. Liu, D. Zhu, B.Z. Tang, Aggregation-induced emission of 1-methyl-1,2,3,4,5-pentaphenylsilole, Chem. Commun. 0 (2001) 1740–1741, https://doi.org/10.1039/B105159H.
[29] Y. Hong, J.W.Y. Lam, B.Z. Tang, Aggregation-induced emission: phenomenon, mechanism and applications, Chem. Commun. 0 (2009) 4332–4353, https://doi.org/10.1039/B904665H.
[30] M. Wang, G. Zhang, D. Zhang, D. Zhu, B.Z. Tang, Fluorescent bio/chemosensors based on silole and tetraphenylethene luminogens with aggregation-induced emission feature, J. Mater. Chem. 20 (2010) 1858–1867, https://doi.org/10.1039/B921610C.
[31] Y. Hong, J.W.Y. Lam, B.Z. Tang, Aggregation-induced emission, Chem. Soc. Rev. 40 (2011) 5361, https://doi.org/10.1039/c1cs15113d.
[32] B.Z. Tang, A. Qin, Aggregation-induced Emission: Fundamentals, John Wiley & Sons, 2013.
[33] M.S. Wong, Z.H. Li, Y. Tao, M. D'Iorio, Synthesis and functional properties of Donor–Acceptor π-conjugated oligomers, Chem. Mater. 15 (2003) 1198–1203, https://doi.org/10.1021/cm0208915.
[34] J.-F. Morin, N. Drolet, Y. Tao, M. Leclerc, Syntheses and characterization of electroactive and photoactive 2,7-carbazolenevinylene-based conjugated oligomers and polymers, Chem. Mater. 16 (2004) 4619–4626, https://doi.org/10.1021/cm0499390.
[35] N. Leclerc, S. Sanaur, L. Galmiche, F. Mathevet, A.-J. Attias, J.-L. Fave, J. Roussel, P. Hapiot, N. Lemaître, B. Geffroy, 6-(Arylvinylene)-3-bromopyridine derivatives as Lego building blocks for liquid crystal, nonlinear optical, and blue light emitting chromophores, Chem. Mater. 17 (2005) 502–513, https://doi.org/10.1021/cm040358k.
[36] E. Gondek, I.V. Kityk, A. Danel, A. Wisla, M. Pokladko, J. Sanetra, B. Sahraoui, Electroluminescence of several pyrazoloquinoline and quinoksaline derivatives, Mater. Lett. 60 (2006) 3301–3306, https://doi.org/10.1016/j.matlet.2006.03.051.
[37] Y. El Kouari, A. Migalska-Zalas, A.K. Arof, B. Sahraoui, Computations of absorption spectra and nonlinear optical properties of molecules based on anthocyanidin structure, Opt. Quant. Electron. 47 (2015) 1091–1099, https://doi.org/10.1007/s11082-014-9965-4.
[38] A.C. Arias, J.D. MacKenzie, I. McCulloch, J. Rivnay, A. Salleo, Materials and applications for large area electronics: solution-based approaches, Chem. Rev. 110 (2010) 3–24, https://doi.org/10.1021/cr900150b.
[39] K.M. Rahulan, S. Balamurugan, K.S. Meena, G.-Y. Yeap, C.C. Kanakam, Synthesis and nonlinear optical absorption of novel chalcone derivative compounds, Opt. Laser Technol. 56 (2014) 142–145, https://doi.org/10.1016/j.optlastec.2013.07.008.
[40] H. Singh, J. Sindhu, J.M. Khurana, Determination of dipole moment, solvatochromic studies and application as turn off fluorescence chemosensor of new 3-(4-(dimethylamino)phenyl)-1-(5-methyl-1-(naphthalen-1-yl)-1H-1,2,3-triazol-4-yl)prop-2-en-1-one, Sens. Actuators B Chem. 192 (2014) 536–542, https://doi.org/10.1016/j.snb.2013.10.137.
[41] Z.R. Grabowski, K. Rotkiewicz, W. Rettig, Structural changes accompanying intramolecular electron transfer: focus on twisted intramolecular charge-transfer states and structures, Chem. Rev. 103 (2003) 3899–4032, https://doi.org/10.1021/cr940745l.
[42] I. Guezguez, A. Ayadi, K. Ordon, K. Iliopoulos, D.G. Branzea, A. Migalska-Zalas, M. Makowska-Janusik, A. El-Ghayoury, B. Sahraoui, Zinc induced a dramatic enhancement of the nonlinear optical properties of an azo-based iminopyridine ligand, J. Phys. Chem. C 118 (2014) 7545–7553, https://doi.org/10.1021/jp412204f.
[43] A. Karakas, A. Migalska-Zalas, Y. El Kouari, A. Gozutok, M. Karakaya, S. Touhtouh, Quantum chemical calculations and experimental studies of third-order nonlinear optical properties of conjugated TTF–quinones, Opt. Mater. 36 (2013) 22–26, https://doi.org/10.1016/j.optmat.2013.07.005.
[44] T.H.N. Pham, R.J. Clarke, Solvent dependence of the photochemistry of the styrylpyridinium dye RH421, J. Phys. Chem. B 112 (2008) 6513–6520, https://doi.org/10.1021/jp711694u.
[45] Y. Huang, T. Cheng, F. Li, C.-H. Huang, T. Hou, A. Yu, X. Zhao, X. Xu, Photophysical studies on the mono- and dichromophoric hemicyanine dyes I. Photoelectric conversion from the dye modified ITO electrodes, J. Phys. Chem. B 106 (2002) 10020–10030, https://doi.org/10.1021/jp020876n.
[46] M. Shaikh, J. Mohanty, P.K. Singh, A.C. Bhasikuttan, R.N. Rajule, V.S. Satam, S.R. Bendre, V.R. Kanetkar, H. Pal, Contrasting solvent polarity effect on the photophysical properties of two newly synthesized aminostyryl dyes in the lower and in the higher solvent polarity regions, J. Phys. Chem. A 114 (2010) 4507–4519, https://doi.org/10.1021/jp9107969.
[47] A.A. Gabr, Spectrophotometric studies on some Schiff bases derived from benzidine, Spectrochim. Acta Part Mol. Spectrosc. 46 (1990) 1751–1757, https://doi.org/10.1016/0584-8539(90)80247-V.
[48] M.J. Wirth, Solvation effects on spectroscopic measurements, TrAC Trends Anal. Chem. 1 (1982) 383–386, https://doi.org/10.1016/0165-9936(82)88008-4.
[49] A.K. Mishra, S.K. Dogra, Effect of solvents and pH on the absorption and fluorescence spectra of 2-phenylbenzimidazole, Spectrochim. Acta Part Mol. Spectrosc. 39 (1983) 609–611, https://doi.org/10.1016/0584-8539(83)80033-6.
[50] S. Song, J. Chen, W. Pan, H. Song, H. Shi, Y. Mai, W. Wen, LED based on alternating benzene-furan oligomers, Spectrochim. Acta A Mol. Biomol. Spectrosc. 170 (2017) 157–166, https://doi.org/10.1016/j.saa.2016.07.008.
[51] A.T.R. Williams, S.A. Winfield, J.N. Miller, Relative fluorescence quantum yields using a computer-controlled luminescence spectrometer, Analyst 108 (1983) 1067–1071, https://doi.org/10.1039/AN9830801067.
[52] S. Dhami, A.J.D. Mello, G. Rumbles, S.M. Bishop, D. Phillips, A. Beeby, Phthalocyanine fluorescence at high concentration: dimers or reabsorption effect? Photochem. Photobiol. 61 (1995) 341–346, https://doi.org/10.1111/j.1751-1097.1995.tb08619.x.
[53] J.L. Bredas, R. Silbey, D.S. Boudreaux, R.R. Chance, Chain-length dependence of electronic and electrochemical properties of conjugated systems: polyacetylene, polyphenylene, polythiophene, and polypyrrole, J. Am. Chem. Soc. 105 (1983) 6555–6559, https://doi.org/10.1021/ja00360a004.
[54] M.-M. Duvenhage, M. Ntwaeaborwa, H.G. Visser, P.J. Swarts, J.C. Swarts, H.C. Swart, Determination of the optical band gap of Alq3 and its derivatives for the use in two-layer OLEDs, Opt. Mater. 42 (2015) 193–198, https://doi.org/10.1016/j.optmat.2015.01.008.
[55] M.J. Frisch, G.W. Trucks, H.B. Schlegel, G.E. Scuseria, M.A. Robb, J.R. Cheeseman, G. Scalmani, V. Barone, G.A. Petersson, H. Nakatsuji, X. Li, M. Caricato, A. Marenich, J. Bloino, B.G. Janesko, R. Gomperts, B. Mennucci, H.P. Hratchian, J.V. Ortiz, A.F. Izmaylov, J.L. Sonnenberg, D. Williams-Young, F. Ding, F. Lipparini, F. Egidi, J. Goings, B. Peng, A. Petrone, T. Henderson, D. Ranasinghe, V.G. Zakrzewski, J. Gao, N. Rega, G. Zheng, W. Liang, M. Hada, M. Ehara, K. Toyota, R. Fukuda, J. Hasegawa, M. Ishida, T. Nakajima, Y. Honda, O. Kitao, H. Nakai, T. Vreven, K. Throssell, J.A. Montgomery Jr., J.E. Peralta, F. Ogliaro, M. Bearpark, J.J. Heyd, E. Brothers, K.N. Kudin, V.N. Staroverov, T. Keith, R. Kobayashi, J. Normand, K. Raghavachari, A. Rendell, J.C. Burant, S.S. Iyengar, J. Tomasi, M. Cossi, J.M. Millam, M. Klene, C. Adamo, R. Cammi, J.W. Ochterski, R.L. Martin, K. Morokuma, O. Farkas, J.B. Foresman, D.J. Fox, Gaussian 09, Revision A.02, Gaussian, Inc., Wallingford CT, 2016.
[56] A.D. Becke, Density-functional thermochemistry. III. The role of exact exchange, J. Chem. Phys. 98 (1993) 5648, https://doi.org/10.1063/1.464913.
[57] C. Lee, W. Yang, R.G. Parr, Development of the Colle-Salvetti correlation-energy formula into a functional of the electron density, Phys. Rev. B 37 (1988) 785–789, https://doi.org/10.1103/PhysRevB.37.785.
[58] W.J. Hehre, R. Ditchfield, J.A. Pople, Self—consistent molecular orbital methods. XII. Further extensions of Gaussian—type basis sets for use in molecular orbital studies of organic molecules, J. Chem. Phys. 56 (1972) 2257–2261, https://doi.org/10.1063/1.1677527.
[59] P.C. Hariharan, J.A. Pople, The influence of polarization functions on molecular orbital hydrogenation energies, Theor. Chim. Acta 28 (1973) 213–222, https://doi.org/10.1007/BF00533485.
[60] Avogadro: an open-source molecular builder and visualization tool. Version 1.2.0 http://avogadro.cc/
[61] M.D. Hanwell, D.E. Curtis, D.C. Lonie, T. Vandermeersch, E. Zurek, G.R. Hutchison, Avogadro: an advanced semantic chemical editor, visualization, and analysis platform, J. Cheminf. 4 (2012) 17, https://doi.org/10.1186/1758-2946-4-17.
[62] J. Tomasi, M. Persico, Molecular interactions in solution: an overview of methods based on continuous distributions of the solvent, Chem. Rev. 94 (1994) 2027–2094, https://doi.org/10.1021/cr00031a013.